CHITOSAN/ BIPHASIC CALCIUM PHOSPHATE NANOFIBROUS SCAFFOLDS FOR BONE TISSUE ENGINEERING

Truong Le Bich Tram

The University of Danang; tlbtram@ac.udn.vn

Abstract - In this article, chitosan/biphasic calcium phosphate (CS/BCP) nanofibers were prepared by electrospinning. From the culture of osteogenic cells, the biocompatibility of CS/BCP nanofibrous substrates was identified and increased by the photocrosslinking. The enhancement in cell attachment and proliferation was caused by the improvement in nanofibers' mechanical properties. The biocompatibility to osteoblasts was also promoted with the content of BCP. The osteogenic differentiation in early, middle and late stage was encouraged by the addition of BCP on nanofibrous substrates. The CS/BCP nanofibers were highly specific to osteogenic cells, revealed by difficulties in the growth of non-osteogenic cells on this composite nanofibrous scaffold. The novel nanofibrous scaffolds showed great potential in the tissue engineering of bones.

Key words - nanofibers; chitosan/ biphasic; osteogenic cells; photocrosslinking; the tissue engineering of bones.

1. Introduction

Research on biomaterials for bone regeneration and replacement has expanded considerably over the last few decades. The implanted biomaterial for bone regeneration should be biocompatible, osteoconductive, with suitableporosity and biomechanical compatibility [1]. The autografts are highly efficient to promote bone generation due to its high osteoconductivity; however, the additional surgery, donor pain and inadequate supply are serious problems in autografts [2]. Allograft is not so limited integration with the surrounding host bone, fragmentation and displacement [3-5]. Accordingly, alloplastic material would be a potential choice and is likely to be widely used clinically but its biocompatibility and osteoconductivity must be improved. Recent advances in nanotechnology allowed the design of materials with nanostructure similar to that of natural bones, which would promote materials' biocompatibility. For example, nanofibers have been applied in bone tissue engineering. One of the most successful methods for producing nanofibres is the electrospinning.

Electrospun CS/BCP composites, composed of an organic phase of polysaccharide and an inorganic phase of calcium phosphate, was possibly served as bioactive tissue-engineered bone scaffolds by mimicking the mechanical properties and regenerative capacity of periosteum while facilitating osteoblast migration from the scaffold/tissue interface. In addition, by mimicking the architectural structure of mature bone, these composite scaffolds would also enhance the differentiation capacity and ECM deposition of osteogenic precursor cells, acting as a bio-template upon which new bone can be formed.

Although CS/BCP nanofibers would be greatly biocompatible and osteoconductive, their high specific surface area as well as high hydrophilicity also results in fast swelling. That is to say, the nano-structures would be damaged in a very short period in vitro or in vivo. Crosslinking of electrospun polymers fibers is thus needed to prevent possible dissolution or erosion of nanofibers. The mechanical properties of nanofibrous substrates would be enhanced by crosslinking, too. Many crosslinkers have been reported to stabilize structures of nanofibers, such as glutaraldehyde (GA) [6], genipin [7], diisocyanates [8] and epoxides [9]. However, most of them showed cytotoxicity [10]. Besides, crosslinking in aqueous solution may damage fiber structures before fibers are fully crosslinked. Photo-crosslinking has recently emerged as a focus of interest in a lot of fields. Compared with traditional crosslinking methods, photocrosslinking is able to easily crosslink electrospun fibers in a one-step process without using additional organic solvents or water, suggesting good retention of fiber morphology and uniformility. The photocrosslinking process is also not cytotoxic and can keep the biofunctionality of materials [11].

In this study, photocrosslinked electrospun CS/BCP nanofibers were fabricated. By culturing osteoblasts, the biocompatibility and bioactivity of CS/BCP nanofibrous scaffolds were explored in this research.

2. Experiment

2.1. Materials

Dihydrogenphosphate (H_2PO_4) 98%, Polyethylene glycol (PEG) with molecular weight 8000 Da, Chitosan (low molecular weight with a degree of deacetylation 75-85%), Trifluoro acetic acid (TFA) 99%, Acetic acid min 99.8%, Tetraethylene glycol diacrylate (TTEGDA), 2,2-Dimeththoxy-2-phenylacetophenone (DMPA) 99%, Sodium carbonate 99.8%, Glycine 99%, were purchased from Sigma-Aldrich. All other solvents and analytical reagents were purchased from commercial suppliers and used as received.

2.2. Preparation of BCP particles

Exact amounts of dihydrogenphosphate (1.25g), calcium hydroxide (0.85g), and PEG (4g) were measured and dissolved in 30 ml de-ionized water and heated to 65°C to facilitate PEG dissolution. The mixture was stirred for 30 min at 300 rpm, producing a milky gel suspension. This gel was then placed in a furnace and heated from 500-1000°C for 30 min under normal atmospheric conditions. This process produced a BCP powder. The entire synthesis experiment was then repeated under the same conditions while excluding PEG.

2.3. Preparation of Photo-crosslinked Electrospun Chitosan/ Biphasis Calcium Phosphate (CS/BCP) nanofibers

2.3.1. Preparation and electrospinning of CS/BCP nanofibers

CS (low molecular weight) solution with

concentrations of 80 mg/ml in co-solvent system of Trifluoroacetic acid (TFA) and Dichloromethane (DCM) (7/3 vol/vol). BCP-containing scaffolds were generated by mixing BCP with CS solution, where the weight ratio of BCP to CS was 2/10. The solution was stirred 250 rpm and the temperature was maintained in 320C overnight. Then, the BCP/CS solution was added into 3cc thermo syringe and placed in electrospinning pump.

The CS/BCP nanofiber were later deposited on stagnant collector of aluminum foil and on 1x1 cm2 cover glass slips. Then CS/BCP nanofibers were dried in surrounding environment condition for overnight before futher characterization. The humidity of the sample was maintained around 40-60%.

2.3.2. Electrospinning of photo-crosslinked CS/BCP solutions

CS/BCP solution with concentrations of CS of 80 mg/ml and BCP of 20%wt/wt in co-solvent system of TFA/DCM (7/3 vol/vol). Perior to the electrospinning process (2-6 hours), photo-crosslinker of Tetraethylene glycol diacrylate (TTEGDA) and 2,2-Dimeththoxy-2-phenylacetophenone (DMPA) were added into the CS/BCP solution. Then, the solution was stirred for 5-6 hours until the solution was homogeneous. The CS/BCP/crosslinker solution was loaded into a 3cc therumo to which a 21-gauge Precision Glide needle was attached. The syringe was then placed on an advancement pump, set at 0.2 ml/h flow rate and a distance of 12 cm from the collecting plate of aluminium foil. A high voltage supply was connected to the needle (positive electrode) and the plate. A voltage of 18 kV was applied. The set-up was run at 23–30°C.

In this study, the photo-crosslinked agent concentration of TTEGDA was varied (0-3-5% wt) while the concentration of photoiniator DMPA remains stable of 1.5%wt, all in the weight percentage based on the total CS concentration.

2.4. Biocompatibility and osteoconductivity analysis

2.4.1. Cells type

The cells cultured in this research include Mouse bone marrow cell (7F2), Mouse Fibroblast cell (L929), and Gingival Fibroblast

2.4.2. Cells Culture

This study used HO-MEM, a modified Eagle's minimal essential medium with Spinner's salts and 10% fetal calf serum, as culture medium for 7F2 cells. In HO-MEM medium preparation, fetal bovine serum (FBS) was added until reaches 10% of total volume as well as penicilin-streptomycin-amphotercin was added until 1% of total volume. When cells were added to the medium, they were incubated at constant temperature of 37^0C in 5% CO_2 environment. When cell proliferation reaches 80% confluence in the flash, the medium was removed and cell were washed by PBS two times. Then, 5 ml of 0.025% trypsin EDTA was added to detach the cells and incubated for 4-5 minutes in 370C with 5% CO_2. When completed, 5 ml medium was added and mixed until total 10 ml solution becomes homogeneous.

2.4.3. Cells Counting

Hemocytometer is a device composed of counting champer used for determining the number of cells per unit volume of a suspension cell. There are two chambers in the hemocytometer, upper side and lower side. Both sides consist of 4 sizes of square at depth of 0.1 mm.

Cells are counted in the bold square and total numbers of cells were calculated. Measurement of cell numbers in replaced by at least three replicates for each parameter. The number of cell in each ml of sollution are calculated by equation:

$$\frac{\sum_1^4 N}{n} \times 2500 \times Dilutionfactor = cellnumber/ml$$

2.4.4. Cell adhesion

Membranes with a size of 1 cm x 1 cm (on cover glass) were neutralized to neutral pH, placed in a 24-well plate, sterilized overnight and the 7F2 cells were placed on each membrane at a density 5000 cells/ml. The cell-seeded scaffolds were maintained in an incubator at 37°C with 5% CO_2. The medium was renewed every 2 days. At a specific time, cells were harvested, washed in PBS two times, fixed in 0.2% GA for 10 min and 2.5% GA for overnight, washed in PBS 3-5 times by DI water, dehydrated through a series of graded ethanol solution in 30%, 50%, 70%, 80%, 90%, 95%, and 99.9 % ethanol for 10 min each, and then dried in a critical point dryer (CPD) (Samdri®-PVT-3D, Tousimis, Inc., USA). Cell attachment and proliferation were observed by SEM.

2.4.5. MTT (3 - (4, 5- dimethylthiazol-2-yl) - 2, 5 - diphenyltetrazolium bromide) assay

Cell viability was evaluated by the reduction of MTT into a formazan dye by living cells. Scaffolds with cultured cell were rinsed by PBS two times, and then were transferred into new 24-well plates containing 1 ml working solution. After incubation 6 h, the working solutions were replaced by DMSO. After being stirred for 15 min, the solution was put into a 96-well plate. An ELISA-plate reader (MQX200R, Bio-Tek Instrument Inc., USA) was used to determine the absorbance at a wavelength of 570 nm.

2.4.6. Alkaline phosphatase (ALPase) assay

ALPase is an early marker for cell differentiation toward the ossteocytic phenotype. Murine 7F2 osteoblast cells were seeded on scaffolds in 24 well plates at density of 5000 cells/ml. ALPase buffer containing 1 mg/ml pNPP was prepared by dissolving the following reagents in deionic water: $MgCl_2$ (1 mM), $ZnCl_2$ (1 mM), and glycine (0.1 M). At each time point, after removing the culture medium, scaffolds with 7F2 cells were washed twice with PBS, immersed into 0.4 ml lysis buffer for 15 min, and put into 1.2 ml of ALPase buffer for 30 min. The reaction was stopped by adding 0.3 ml 3N NaOH. Next, the absorbance was read at 405 nm using an ELISA plate reader. Total protein was measured by bicinchoninic acid (BCA) assay. For this assay, lysis containing UMR cells and BCA working agent were well mixed and placed in a 96-well plate. The plate was kept at 37°C for 2 hours. The absorbance

was determined at 562 nm using a ELISA plate reader.

2.4.7. Osteogenic Differentiation

When osteoprogenitors start to differentiate into osteoblast, in the early state they will secrete genetic markers such as collagen type I (COL I), alkaline phosphatase (ALPase), osteopontin (OPN). In the final state they will secrete bone sialoprotein (BSP) and osteocalcin (OCN). They were conducted under process follow:

After 1, 3, 5, 7 and 9 days of cultivation, all cells on scaffolds were digested with trypsin–EDTA. Total cellular RNA was isolated by lysis in TRIzol (Invitrogen). The levels of bone-specific genes, including COL I, BSP, ALPase, and OCN of cells cultured on CS and CS/BCP nanofibrous scaffolds were assessed by real-time PCR. The mRNA level of glyceraldehyde-3-phosphate dehydrogenase (GAPDH) was used as internal control. Real-time PCR was performed using a Brilliant SYBR Green QPCR Master Mix (TakaRa). The PCR cycling consisted of 40 cycles of amplification of the template DNA with primer annealing at 60 °C. The relative level of expression of each target gene was then calculated using the delta-delta Ct method. The amplification efficiencies of primer pairs were validated to enable quantitative comparison of gene expression. All primers (Invitrogen) were designed using primer 5.0. Target genes were normalized to GAPDH.

3. Results and discussion

3.1. Viability of osteoblasts on CS/BCP nanofibers with various photo-crosslinker concentrations

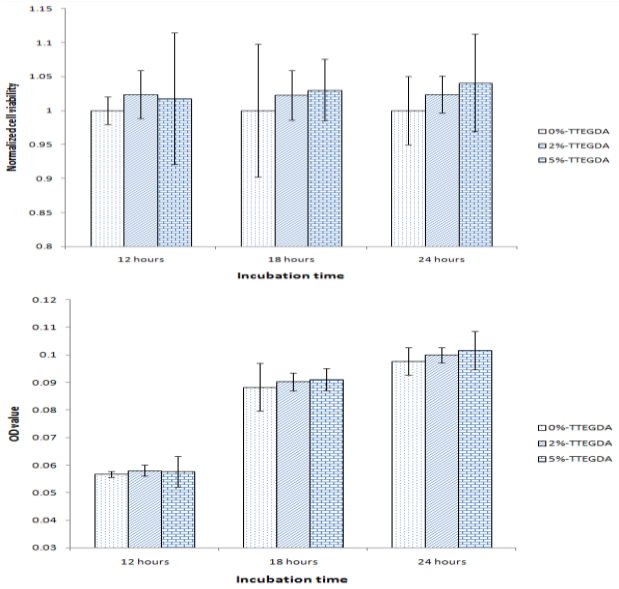

Figure 1. *The 7F2 viability on CS/BCP nanofibers with different photo-crosslinker concentrationsin the beginning of incubation. The OD value was normalized (a) and non-normalized (b) by the cell viability on CS/BCP without TTEGDA (0%-TTEGDA). Initial cell seeding density was 5000 cells/ml (n=3)*

The 7F2 cells were cultured on photo-crosslinked CS/BCP nanofibers with various TTEGDA concentrations and the results of cell viability at the beginning of culture were presented in Figure 1. Within culture for 1 day, the viability of osteoblast increased with TTEGDA concentration, revealed by 5%-TTEGDA > 2%TTEGDA > 0%TTEGDA.The results from Figure 1 support that the biocompatibility of CS/BCP nanofibers was enhanced by photo-crosslinking and the enhancement was more significant when corsslinking degree was higher. The improvement in biocompatibility due to photo-crosslinking was possibly caused by the enhancement in the mechanical properties of CS/BCP nanofibers. The nanofibers with good mechanical strength can efficiently support the lamallipodia extrusion, and thus promote the formation of stable array of elongated focal adhesion and increase tyrosine of focal adhesion kinase (FAK) [12].

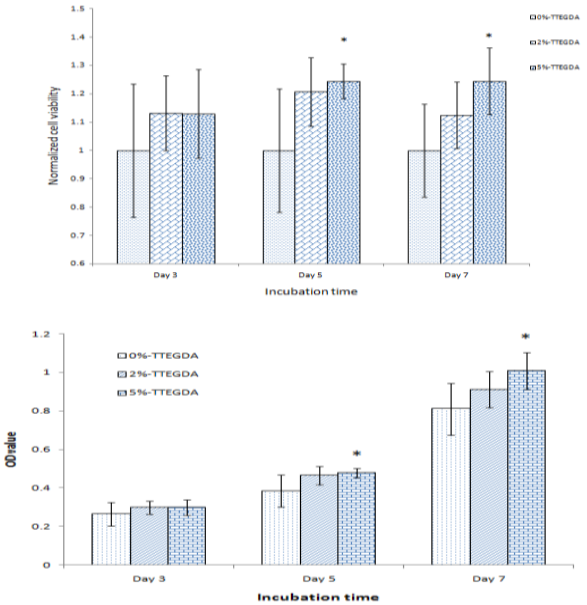

Figure 2. *The viability of 7F2 on CS/BCP nanofibers with different photo-crosslinker concentrations for long incubation periods. The OD value was normalized (a) and non-normalized (b) by the cell viability on CS/BCP without any treatment (0%-TTEGDA). Initial cell seeding density was 5000 cells/ml. By t-test, * indicates significant difference compared with CS/BCP nanofibers containing 0% of TTEGDA, and + indicates significant difference between indicated samples. (*/+ indicates p<0.2, n=3)*

Figure 2 shows the cellular viability on photocrosslinked CS/BCP fibers for long incubation periods (3, 5 and 7 days). The cell viability on nanofibers with photocrosslinking was higher than those without crosslinking. The results at 5th and 7th day further indicate that the cell activity increased with the concentration of TTEDGA. The outcome proves that the photocrosslinking process developed in this research efficiently promote nanofibers' biocompatibility. This was due to the enhancement in the mechanical strength of CS/BCP composite nanofibers in aqueous conditions. In comparison with Ko et al.'s study, they used genipin to crosslingk CS nanofibers [13]. Their results showed that the crosslinking with 0.5% (w/v) genipin enhanced nanofibers' biocompatibility, but this enhancement was limited, compared with the findings in this research.

Rnjak et al.'s researches also showed for CS nanofibers, the crosslinking processes by using GA was not as efficient on promoting cell viability as the photocrosslinking process developed in this study. The above results and comparisons reveal that the photocrosslinking was not only convenient but also highly potential [14].

3.2. Osteogenic differentiation of Osteoblasts on CS/BCP nanofibers with various photo-crosslinker concentration

Figure 3 shows ALPase expression of cultured osteoblasts on photocrosslinked CS/BCP nanofibers with different TTEGDA concentrations. After the culture for 5 days, the ALPase expression became significant on every kind of nanofibers, meaning the initiation of early osteogenic differentiation. On photocrosslinked nanofibes, ALPase activity was apparently higher than that onun-crosslinked nanofibes, 0%-TTEGDA, and increased with the concentration of TTEGDA. This result would be explained by the mechanical properties stabilized by the photocrosslinking process. By increasing TTEGDA concentration, the mechanical strength of CS/BCP in aqueous conditions was enhanced, whichpromoted not only cell viability but also the following ALPase expression. The result demonstrates that the osteoconductivity of CS/BCP nanofibers in early differentiation stage was able to be promoted by photocrosslinking proposed in this study. The enhancement in early osteogenic differentiation due to the promotion of mechanical strength was in line with previous findings [15].

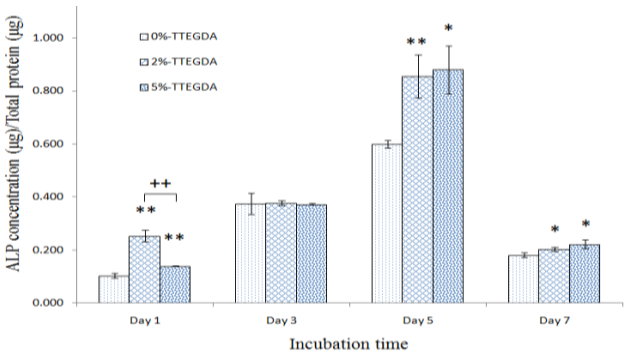

Figure 3. *The ALPase activities on crossliked electrospun CS/BCP nanofibers with different photo-crosslinker concentrations for long incubation periods. Initial cell seeding density was 5000 cells/ml. By t-test, * indicates significant difference compared with CS/BCP nanofibers containing 0% TTEGDA, and + indicates significant difference between two indicated samples. (*/+ indicates p<0.05, **/++ indicates p<0.01, n=3)*

3.3. Biocompatibility and osteoconductivity of CS/BCP nanofibers on 7F2 Osteoblasts with various BCP concentrations

Proliferation of 7F2 cells on the nanofibrous scaffolds of CS/BCP and CS after the culture for 1, 3, and 5 days were determined using MTT assay and the results are presented in Figure 4. There was no significant difference in cell viability on nanofibrous scaffold with different contents of BCP on the first day, which was because BCP were encapsulated inside CS nanofibers and it would take time to release calcium ions. Thus, BCP was not effective yet on the 1st day. After the culture for 3 and 5 days, the blending with BCP significantly promoted the biocompatibility of CS nanofibers, and the cell viability was basically increased with BCP amounts. The results prove that electrospun nanofibrous CS/BCP scaffolds significantly encouraged the proliferation of osteoblasts. The viability of 7F2 cells on the CS/BCP composite nanofibers slightly decreased when the BCP content attained 40%. The finding suggests that if the BCP concentration was too high, the viability of osteoblast would be suppressed instead of being encouraged. The toxicity to osteoblasts from over-released calcium ions was also reported in previous studies [16].

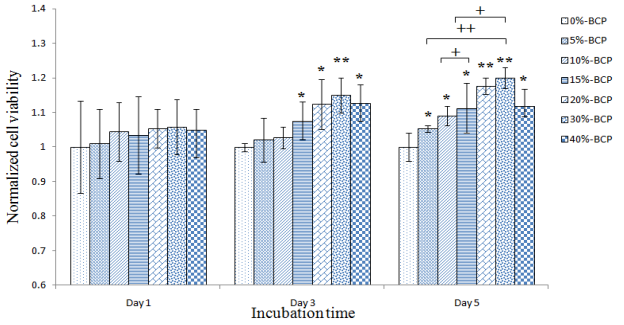

Figure 4. *The 7F2 cell viability on photocrosslinked CS/BCP nanofibers with different BCP concentrations. The OD value was normalized by the cell viability on pure CS nanofibers. Initial cell seeding density was 5000 cells/ml. By t-test, * indicates significant difference compared with CS/BCP nanofibers containing 0% BCP, and + indicates significant difference between two indicated samples. (*/+ indicates p<0.1, **/++ indicates p<0.01, n=3)*

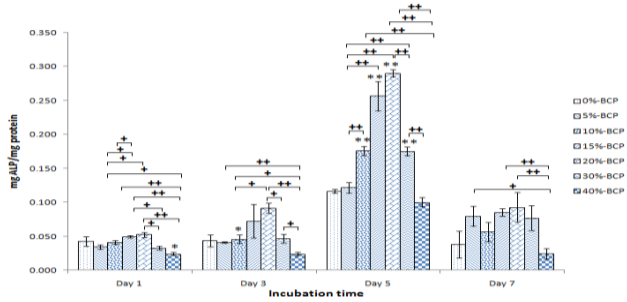

Figure 5. *The ALPase activities on crosslinked electrospun CS/BCP nanofibers with different BCP concentrations for long incubation periods. Initial cell seeding density was 5000 cells/ml. By t-test, * indicates significant difference compared with pure CS nanofibers containing 0% BCP, and + indicates significant difference between two indicated samples. (*/+ indicates p<0.01, **/++ indicates p<0.001, n=3)*

Figure 5 illustrates the ALPase activity of cells cultured on crosslinked nanofibers with different amounts of BCP. Compared with cells on pure CS substrates, 7F2 cultured on CS/BCP composites showed a higher ALPase level except for those with BCP more than 20wt%. The improvement of ALPase activity was particularly remarkable when nanofibers contained 15-20 wt% BCP. This enhancement suggested that the presence of the BCP promote the early osteogenic differentiation because BCP was osteoconductive. The result was in agreement with previous observations forgelatin/HA and collagen/

biocomposites where the adhesion and proliferation were enhanced by incorporating a suitable amount of calcium phosphates [17].

Compared with results from cell viability in Figure 4, the effects of BCP were roughly the same; that was, the ALPase activity increased with BCP contents in a suitable range. However, BCP of 30 wt% can still enhance the viability of 7F2 but not so effective on promoting ALPase expression. The results show that the limitation of BCP amounts would be different in stimulating the proliferation and differentiation of osteogenic cells.

3.4. Biocompatibility of CS/BCP membranes on L-929 Fibroblasts with various BCP concentration

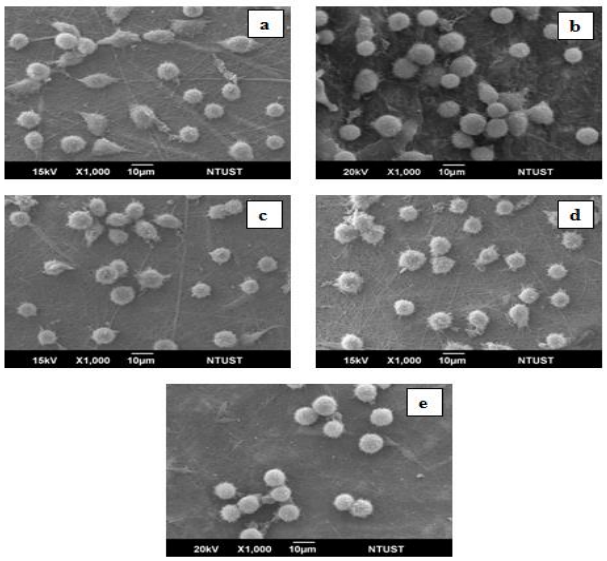

Figure 6. *SEM images of L-929 cells after the cultivation for one day on photocrosslinked electrospun CS/BCP nanofibers with different BCP contents: (a) 0% BCP, (b) 10% BCP, (c) 20% BCP, (d) 30% BCP and (e) 40% BCP*

The morphologies of L-929 cells, fibroblasts isolated from muscle tissue, cultured on photocrosslinked electrospun CS and CS/BCP nanofibers with various BCP concentrations are shown in Figures 6 to 10. After 1-day incubation, the cells were still round on nanofibrous CS/BCP (Figure 6(c)-(e)), while some cells spread on CS nanofibers (Figure 6(a)). After the culture for 3 days, the number of spread cells on CS nanofibers (Figure 7(a)) was much more than that on CS/BCP nanofibers (Figure 7(c)-(e)). After the incubation for 5 days, some cells spread on CS/BCP nanofibers while almost all the cells completely spread on CS nanofibers (Figure 8). After 7 days, most cells completely spread on nanofibrous CS as well as on CS/BCP nanofibers (Figure 9). From the SEM pictures, the L-929 cells, a non-osteogenic cell, exhibited quick attachment and spreading on CS nanofibers but not on CS/BCP nanofibers. In fact, the attachment of L929 was suppressed more with higher content of BCP. The above tendency was totally opposite to what we found for osteoblasts, revealing that the nanofibers would be highly specific to osteogenic cells by incorporating with BCP. The cell-selectivity of BCP was indicated in Baxter et al.'s study [18]; however, this was the first study to fabricate composite biomaterials specific to osteogenic cells by blending with BCP.

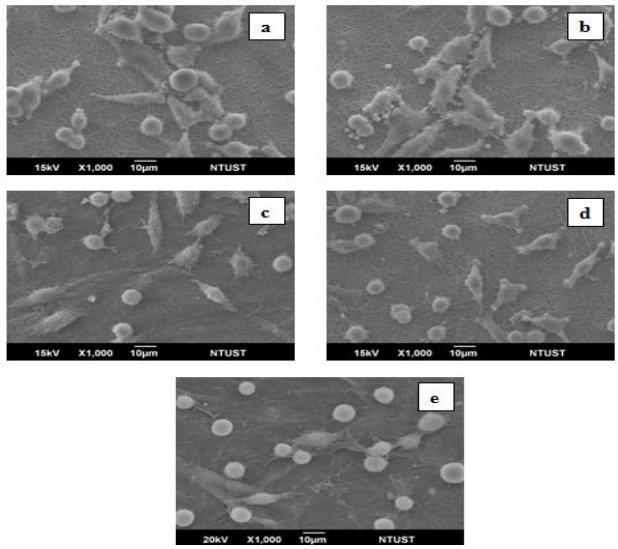

Figure 7. *SEM images of L-929 cells after the cultivation for 3 days on photocrosslinked electrospun CS/BCP nanofibers with differentBCP contents: (a) 0% BCP, (b) 10% BCP, (c) 20% BCP, (d) 30% BCP and (e) 40% BCP*

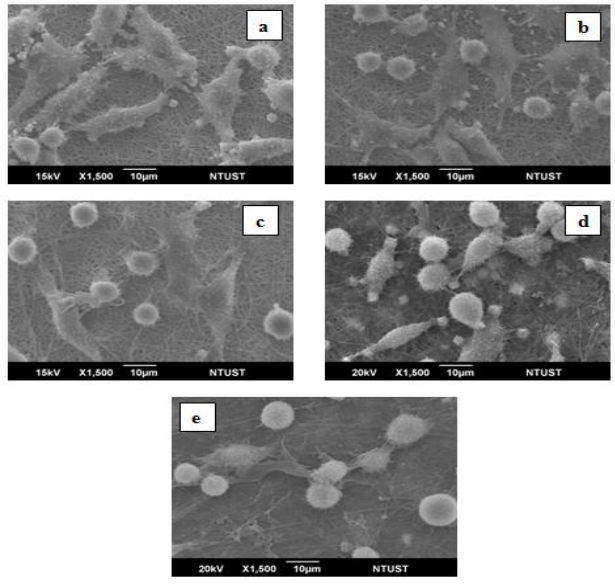

Figure 8. *SEM images of L-929 cells after cultivation for 5 days on photocrosslinked electrospun CS/BCP nanofibers with different BCP contents: (a) 0% BCP, (b) 10% BCP, (c) 20% BCP, (d) 30% BCP and (e) 40% BCP*

The details in cell morphologies were observed from magnified SEM images in Figure 10. Based on Figure 10(a), on scaffolds without BCP, fibroblasts well interact and elongate along fibers with multiple directions. Furthermore, the cell directionality exhibits great deviations from the underlying fiber alignment due to the high likelihood interaction of cell lamellipodia with multiple, rather than single, nanofibers. On the contrary, 7F2 cultured on electrospun nanofibers containing BCP with high contents showed almost no fillapodia or lamellipodia. Even worse, Figure 10(b) suggests that the cultured fibroblasts were damaged by BCP with high content. The results emphasize the cell-selectivity of CS/BSP composite and the cytotoxicity of

composite nanofibers with great amount of BCP to non-osteogenic cells.

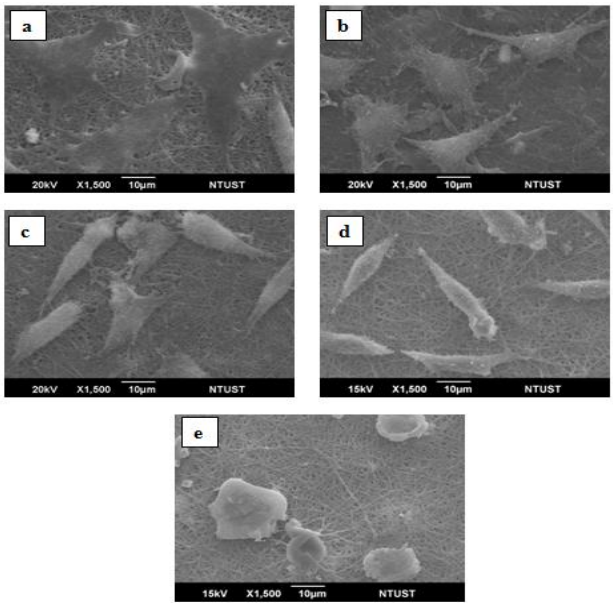

Figure 9. *SEM images of L-929 cells after cultivation for 7 days on photocrosslinked electrospun CS/BCP nanofibers with differentBCP contents: (a) 0% BCP, (b) 10% BCP, (c) 20% BCP, (d) 30% BCP and (e) 40% BCP*

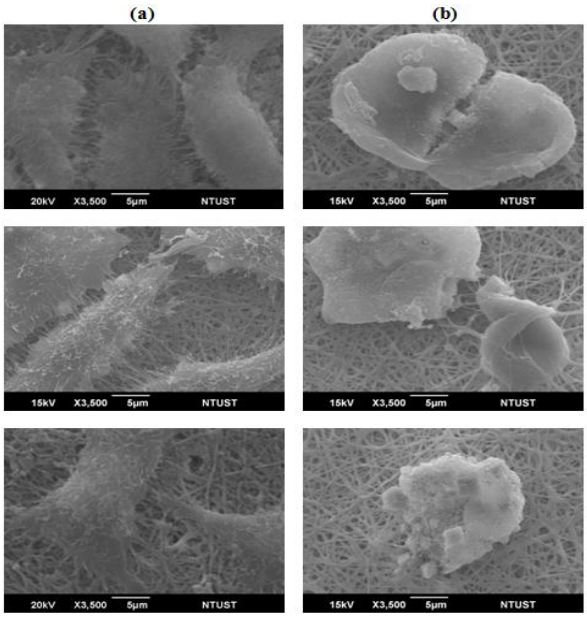

Figure 10. *SEM images of L-929 cells on photo-crosslinked pure CS nanofiber (a) and CS/BCP nanofibers with 40% BCP (b)*

The viability of L929 cells were quantified by MTT assay and the results were presented in Figure 11. Although there was no significant difference caused by BCP blending on the 1st day, the cell viability decreased with BCP contents after the culture for 3 and 5 days. The results show that the cytotoxicity to non-osteogenic cells increased with the concentration of BCP, which was in line with the findings from Figures 6 to 10 and was contrary to the tendency for osteoblasts. It is proved that CS/BCP nanofibers would be highly specific to osteogenic cells, especially when the BCP content was high enough.

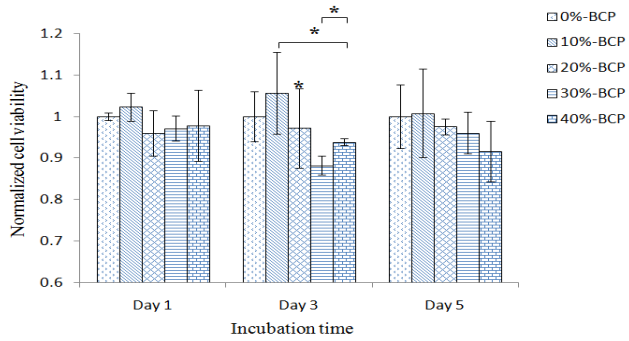

Figure 11. *The L-929 viability on CS/BCP nanofiberswith different BCP concentrations. The OD value was normalized by the cell viability on CS scaffold without BCP. Initial cell seeding density was 5000 cells/ml. By t-test, * indicates significant difference compared with CS nanofibers containing 0% of BCP, and + indicates significant difference between two indicated samples. (*/+ indicates p<0.1, **/++ indicates p<0.01, n=3)*

3.5. Biocompatibility and osteoconductivity of CS/BCP membranes on Gingival Fibroblasts (GF) with various BCP concentration

To further evaluate the cell-selectivity of CS/BCP nanofibers, GF cells with osteogenic and non-osteogenic subgroups were cultured on CS/BCP nanofibrous substrates with various BCP concentrations. From Figure 12, the viability of GF was enhanced by the addition of BCP with the content of 10-30wt%, and 20% BCP was the most effective one. With very high BCP concentration as 30 and 40 wt%, the suppression in cell viability was observed and cell viability decreased with BCP contents. The above two tendencies in conflict with each other would be caused by two different subgroups in GF. The proliferation of osteogenic subgroups in GF was promoted while the proliferation of non-osteogenic cells was inhibited by BCP. This contradict would be especially clear when BCP concentration was high enough.

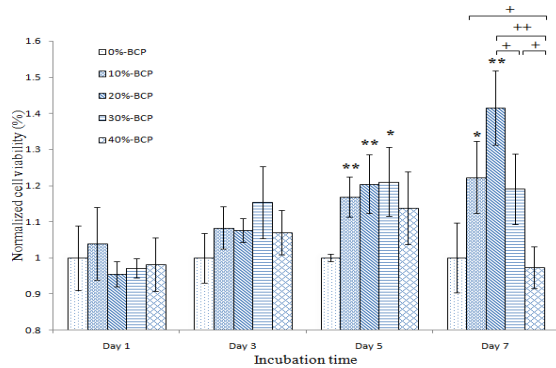

Figure 12. *The viabilityof gingival fibroblasts on photocrosslinked CS/BCP nanofibers with different BCP concentrations. The OD value was normalized by the cell viability on pure CS nanofibers. Initial cell seeding density was 5000 cells/ml. By t-test, * indicates significant difference compared with CS/BCP nanofibers containing 0% BCP, and + indicates significant difference between two indicated samples. (*/+ indicates p<0.05, **/++ indicates p<0.01, n=3)*

Figure 13 shows ALPase expression of GF cells on photocrosslinked CS/BCP nanofibers with different concentration of BCP. In the beginning of culture (day 1), the differences between ALPase expression of GF in each

group were not clear. After culture for 3 and days, the ALPase expressions on nanofibers containing 10% and 20% BCP were apparently higher than those on pure CS nanofibers. From Figure 13, BCP in the composites encouraged the osteoblastic phenotypes of GF. However, when the amount of BCP exceeded 30wt%, the ALPase activities began to decrease. Compared with ALPase expressions of osteoblasts, the reflection point of ALPase activity was the same to be 30wt% BCP. Thus, we interfered that the promotion in ALPase expression caused by BCP was mainly due to the early differentiation of osteogenic subgroup in GF.

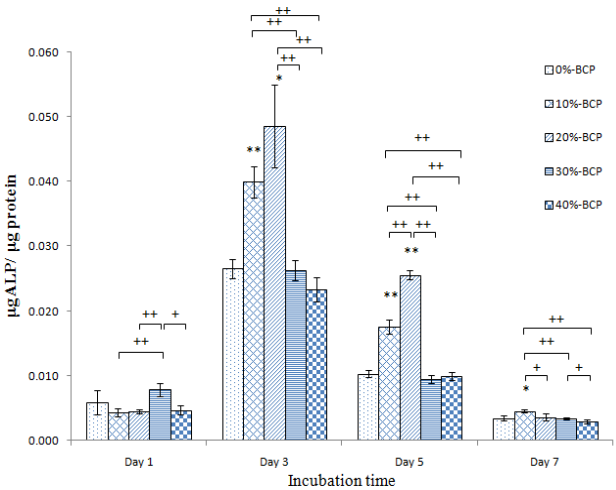

Figure 13. *The ALPase activities of gingival fibroblasts on crossliked electrospun CS/BCP nanofibers with different BCP concentrations for long incubation periods. Initial cell seeding density was 5000 cells/ml. By t-test, * indicates significant difference compared with pure CS nanofibers containing 0% BCP, and + indicates significant difference between two indicated samples. (*/+ indicates p<0.05, **/++ indicates p<0.01, n=3)*

4. Conclusion

In this paper, CS/BCP nanofibers were fabricated via electrospinning process. The results from cellculture shows that the photocrosslinked CS/BCP nanofibers were biocompatibility and the viability of cultured cells were enhanced with the blending with BCP. These results implied that the photocrosslinked CS/BCP electrospun fibers were highly osteoconductive. By culturing osteogenic cells as well as non-osteogenic cells, it was found that CS/BCP was greatly cell-selective especially when the BCP content was high. The osteoblasts proliferate and differentiate well on CS/BCP nanofibrous substrates, while non-osteogenic muscle fibroblasts poorly attach or were even damaged on CS/BCP nanofibers.

Based on these results, electrospun photo-crosslinked CS/BCP nanofibrous scaffolds are proved to be a potential candidate in bone tissue engineering or regeneration due to the biocompatibility, osteoconductivity and cell-selectivity.

REFERENCES

[1] Cenni E., Pizzoferrato A., Ciapetti G., Granchi D., Savarino L., Stea S., "Inflammatory response to metals and ceramics". *Integrated Biomaterials Science*, 2002. p. 735–791.

[2] Wagh A., "Chemically Bonded Phosphate Ceramics: Twenty-First Century Materials with Diverse Applications". *Elsevier Science*, 2004.

[3] Veis A., "Phosphoproteins from teeth and bone". *Ciba Found Symp*, 1998. **136**, p. 161-177.

[4] Songtao Shi, Martin Kirk, Arnold J. Kahn, "The role of type I collagen in the regulation of the osteoblast phenotype". *Journal of Bone and Mineral Research*, 1996. **11**(8), p. 1139-1145.

[5] Boskey AL., Posner AS., "Bone structure, composition, and mineralization". *Orthop Clin North Am*, 1984. **15**(597-612).

[6] Schiffman JD., "Schauer CL., Cross-linking chitosan nanofibers". *Biomacromolecules*, 2007. **8**, p. 594– 601.

[7] Mi FL., Tan YC., Liang HC., Huang RN., Sung HW., "In vitro evaluation of a chitosan membrane cross-linked with genipin". *J. Biomater. Sci. Polym.*, 2001. **12**, p. 835– 850.

[8] Eric R. Schauer Welsh, Santos CL., John PP, Ronald R., "In Situ Cross-Linking of Alternating Polyelectrolyte Multilayer Films". *Langmuir*, 2004. **20**(5), p. 1807-1811.

[9] Wan Ngah WS., Endud CS., Mayanar R., "Removal of copper(II) ions from aqueous solution onto chitosan and cross-linked chitosan beads". *Reactive and Functional Polymers*, 2002. **50**(2), p. 181-190.

[10] Zhang Sisson K., Farach-Carson C., Chase MC., Rabolt DB., "Evaluation of cross-linking methods for electrospun gelatin on cell growth and viability". *Biomacromolecules*, 2009. **10**(7), p. 1675-1680.

[11] Yu Jin, Dongzhi Yang, Yingshan Zhou, Guiping Ma, "Jun Nie, Photocrosslinked electrospun chitosan-based biocompatible nanofibers". *Journal of Applied Polymer Science*, 2008. **109**(5), p. 3337-3343.

[12] Aduba DJ., "Bachelor of science". *Master of Science, Biomedical Engineering*, 2008.

[13] HaiYan Yin, Jong Hyun Ko, Jeongho An, Dong June Chung, Ji-Heung Kim, Soo Bok Lee, Do Gi Pyun, "Characterization of cross-linked gelatin nanofibers through electrospinning". *Macromolecular Research*, 2010. **18**(2), p. 137-143.

[14] Jelena Rnjak Kovacina, Steven G. Wise, Zhe Li, Peter KM. Maitz, Cara J. Young, Yiwei Wang, "Anthony S. Weiss, Tailoring the porosity and pore size of electrospun synthetic human elastin scaffolds for dermal tissue engineering". *Biomaterials*, 2011. **32**(28), p. 6729-6736.

[15] Xuan Cai, Hua Tong, Xinyu Shen, Weixuan Chen, Juan Yan, Jiming Hu, "Preparation and characterization of homogeneous chitosan–polylactic acid/hydroxyapatite nanocomposite for bone tissue engineering and evaluation of its mechanical properties". *Acta Biomaterialia*, 2009. **5**(7), p. 2693-2703.

[16] Hae-Won Kim, Jonathan C. Knowles, Hyoun-Ee Kim, "Hydroxyapatite and gelatin composite foams processed via novel freeze-drying and crosslinking for use as temporary hard tissue scaffolds". *Journal of Biomedical Materials Research Part A*, 2005. **72A**(2), p. 136-145.

[17] Hae-Won Kim, Hyoun-Ee Kim, Vehid Salih, "Stimulation of osteoblast responses to biomimetic nanocomposites of gelatin–hydroxyapatite for tissue engineering scaffolds". *Biomaterials*, 2005. **26**(25), p. 5221-5230.

[18] Frauchiger V., Baxter LC., "Textor M., Gwynn I., Richards RG., Fibroblast and osteoblast adhesion and morphology on calcium phospha te surfaces". *eCM Journal*, 2002. 4, p. 1-17.

(The Board of Editors received the article on 03/5/2020, its review was completed on 18/6/2020)